*International Journal of Thermophysics, Vol. 23, No. 1, January 2002 (© 2002)*

# Total Hemispherical Emittance of Polyimide Films for Space Use in the Temperature Range from 173 to 700 K[1]

**K. Fukuzawa,[2] A. Ohnishi,[3,4] and Y. Nagasaka[2]**

This paper describes the temperature dependence of the total hemispherical emittance $\epsilon_h$ in the temperature range from 173 to 700 K for three types of thermal control materials, which are based on a thin polyimide film coated with aluminum on the back surface. The results obtained from the measurements are compared with calculated values from optical constants. The principle of the present measurement is based on the steady-state calorimetric method, and $\epsilon_h$ is obtained by measuring the equilibrium temperature of a sample corresponding to different heat inputs to a heater attached to the sample. On the other hand, the present calculation method is performed by using data for the optical constants of polyimide films and vapor-deposited metal in the wavelength region from 0.25 to 100 μm. These results agree with each other on the whole. It has been observed that the temperature dependence of $\epsilon_h$ is remarkable, and the values have a maximum around 410 K.

**KEY WORDS:** Mercury orbiter mission; optical constants; polyimide film; steady-state calorimetric method; thermal control materials; total hemispherical emittance.

## 1. INTRODUCTION

There are many thermal engineering problems associated with a scientific exploration mission of Mercury, the innermost and hottest planet in the solar

[1] Paper presented at the Fourteenth Symposium on Thermophysical Properties, June 25–30, 2000, Boulder, Colorado, U.S.A.

[2] Department of Mechanical Engineering, Keio University, 3-14-1, Hiyoshi, Yokohama, 223-8522, Japan.

[3] Institute of Space and Astronautical Science, 3-1-1, Yoshinodai, Sagamihara 229-8510, Japan.

[4] To whom correspondence should be addressed. E-mail: ohnishi@pub.isas.ac.jp



0195-928X/02/0100-0319/0 © 2002 Plenum Publishing Corporation

system. The Mercury orbiter mission spacecraft receives intense illumination, 10 times higher than near Earth, and, at the same time, is exposed to energy radiated from Mercury, whose surface temperature is over 700 K. The harsh thermal environment of Mercury, compared to that of Earth, is presented in Table I [1, 2]. The distance between the sun and Mercury varies from 0.306 to 0.47 AU (astronomical units), so the maximum solar flux intensity around Mercury at the perihelion is about 10.6 times higher than that around Earth. Even at the aphelion, the solar intensity reaches 4.6 times higher. And because of Mercury's low albedo, the maximum infrared intensity from Mercury reaches about 13470 $W \cdot m^{-2}$ at the perihelion, which is over 50 times higher than for an orbit around Earth. Therefore, thermal control materials covering a spacecraft for Mercury exploration are required to withstand the severe thermal environment as well as the widely varying heat flux during the cruising orbit. This paper describes the temperature dependence of the total hemispherical emittance $\epsilon_h$ of three types of thermal control materials based upon polyimide films for space use in the temperature range from 173 to 700 K by means of experimental measurements based on the steady-state calorimetric method and calculations from optical constants.

## 2. THERMAL CONTROL MATERIALS

In general, multilayer insulation (MLI), which consists of many sheets of thermal control films, is used on various spacecraft surfaces as the main passive part of the thermal control. Thermal control films are usually thin polymer films with vapor-deposited metal on the back surface [3]. It is well known that polyimide films are superior in long-term heat resistance, chemical resistance, irradiation resistance, etc., among polymer films. The polyimide films Kapton-H, which is produced from pyromelitic dianhydride and 4,4′-diaminodiphenyl ether (DADE), UPILEX-R (UBE Industries, Ltd.), which is produced from 3,3′,4,4′-biphenyl tetracarboxylic acid dianhydride

**Table I.** Thermal Environment Around the Mercury Orbit [1, 2]

| | Mercury | Earth | Notes |
|---|---|---|---|
| Solar intensity | 6220–14330 $W \cdot m^{-2}$ | 1289–1421 $W \cdot m^{-2}$ | 4.6–10.6 times |
| Albedo (intensity) | 0.06 (373–716 $W \cdot m^{-2}$) | 0.25–0.35 (322–497 $W \cdot m^{-2}$) | |
| Radiative intensity[a] | 5847–13470 $W \cdot m^{-2}$ | 216–258 $W \cdot m^{-2}$ | |

[a] The peak value at right insolation is given for Mercury, while the average value is given for Earth.

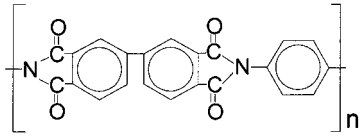

UPILEX-S

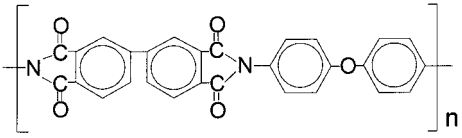

UPILEX-R

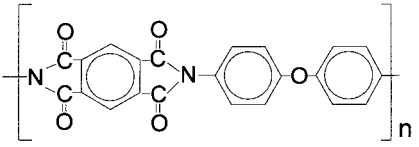

Kapton-H

**Fig. 1.** Chemical structure of polyimide films.

(*s*-BPDA), and DADE have been used on numerous spacecrafts [3, 4]. The polyimide film UPILEX-S (UBE Industries, Ltd.) is generated from *s*-BPDA and *p*-phenylene diamine. UPILEX-S film is superior in long-term heat resistance compared with Kapton-H and UPILEX-R. Chemical structures of polyimide films are shown in Fig. 1. The long-term thermal life of polymer films is usually determined by Arrhenius plots of the tensile strength half-life. The temperature ($T_{20,000}$) corresponding to the half-life extrapolated to 20,000 h of tensile strength in the Arrhenius plots and the glass transition temperature ($T_g$) are listed in Table II [5, 6].

In this paper, the thicknesses of three types of thermal control materials are as follows: UPILEX-S film, 20 μm; UPILEX-R film, 25 μm; and Kapton-H film, 25 μm.

**Table II.** Properties of Polyimide Films [5, 6]

| | Density ($g \cdot cm^{-3}$) | $T_g$ (K) | $T_{20,000}$ (K) |
|---|---|---|---|
| UPILEX-S | 1.47 | 632 | 563 |
| UPILEX-R | 1.39 | 576 | 543 |
| Kapton-H | 1.42 | 700 | 538 |

## 3. MEASUREMENTS

### 3.1. Principle of the Measurements

The principle of the present measurements is based on the steady-state calorimetric method [7]. The total hemispherical emittance $\epsilon_h$ is determined by equating electrical heat input to the sample with radiative heat loss from the sample to the surroundings. Figure 2 shows the energy balance diagram of the sample. The sample is suspended by lead wires and thermocouples inside an evacuated test chamber, the wall of which is coated with a near-black material. The test chamber walls are cooled to a low temperature, while the sample is heated electrically through a sheet heater. It is assumed that $\epsilon_h$ of the sample is equal to the total hemispherical absorbance $\alpha_h$. When the sample temperature $T_S$ is at steady state, then the equation of energy balance can be expressed as follows:

$$Q = \varepsilon_h(T_S)\,\sigma A_S(T_S^4 - T_W^4) + Q_W + Q_g - Q_r \tag{1}$$

where $\sigma$ is the Stefan–Boltzmann constant, $A_S$ is the total surface area of the sample, $T_S$ and $T_W$ are the temperatures of the sample and test chamber wall, $Q$ is the supplied electrical power determined by the electric current

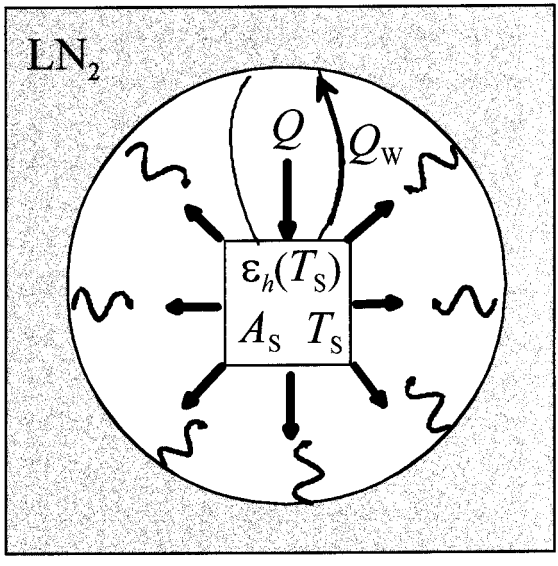


**Fig. 2.** Energy balance diagram.

and the terminal voltage of the sample, $Q_W$ is the heat loss of the sample through the lead wires, $Q_g$ is the heat loss through residual gas, and $Q_r$ is the heat input by multiple reflection between the sample and the test chamber wall.

In the present measurements, since the test chamber is maintained in a high vacuum, and since the surface area of the test chamber is much larger than the total surface area of the sample, $Q_g$ and $Q_r$ are neglected. Therefore, $\varepsilon_h$ is calculated by measuring the supplied electrical power $Q$, the temperature of the sample $T_S$ and the test chamber wall $T_W$, and the total surface area of the sample $A_S$ and estimating the heat loss through the lead wires $Q_W$ as follows:

$$\varepsilon_h(T_S) = \frac{Q - Q_W}{\sigma A_S (T_S^4 - T_W^4)} \tag{2}$$

### 3.2. Experimental Apparatus

Figure 3 shows a schematic drawing of the present experimental apparatus [7]. This system consists of a liquid nitrogen ($LN_2$) cryostat with a test chamber, a port for sample exchange, a system for the up-and-down motion

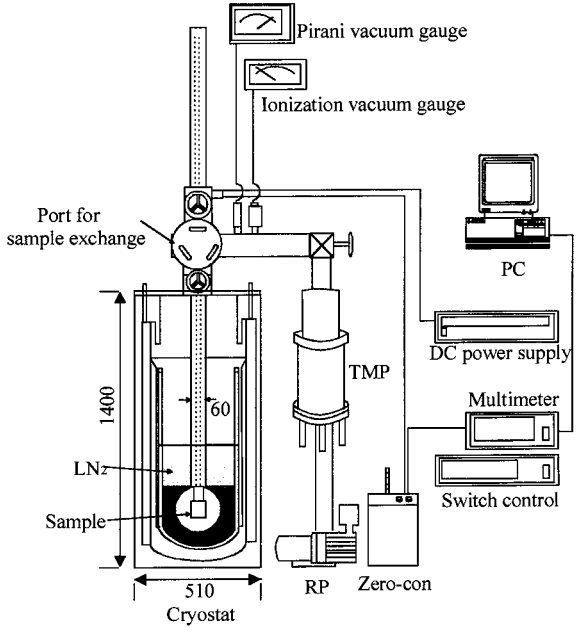


**Fig. 3.** Experimental apparatus.

of the sample, a vacuum system, measuring instruments, and a personal computer, which controls the sample temperature and logs the experimental data. The inside diameter of the spherical test chamber is 250 mm and the inner surface is painted with a near-black paint (CHEMGLAZE Z306) with a very high total hemispherical absorptance. This test chamber is located at the bottom of the liquid nitrogen cryostat, whose diameter is 510 mm and depth is 1400 mm. During the measurement, the test chamber is cooled to 77 K by $LN_2$ and kept under $10^{-5}$ Pa vacuum using a turbomolecular pump.

### 3.3. Sample Structure

The sample structure is shown in Fig. 4. Test samples are made using two pieces of aluminum plates ($20 \times 20 \times 0.5\ mm^3$) and a sandwiched sheet heater. Thermal control films are stuck on the sample plates with heat-resistant glue (KE3417 or KE3418; Shin-Etsu Chemical Co., Ltd). The temperature of the sample is measured by a calibrated chromel–alumel thermocouple (50 μm in diameter), which is attached to the center of the sample with the sheet heater. For the distribution of the surface temperature to be equal, a sheet heater ($19 \times 19\ mm^2$), which has an aluminum heating element ($240 \pm 5\ \Omega$) as shown in Fig. 4, is adopted in the present measurements. Constantan lead wires (50 μm in diameter) in the temperature range from 173 to 373 K and copper lead wires (100 μm in diameter) in the temperature range from 373 to 700 K are adopted and attached to the sheet heater with silver paste (Pyro-Duct 597; Aremco Products, Inc.).

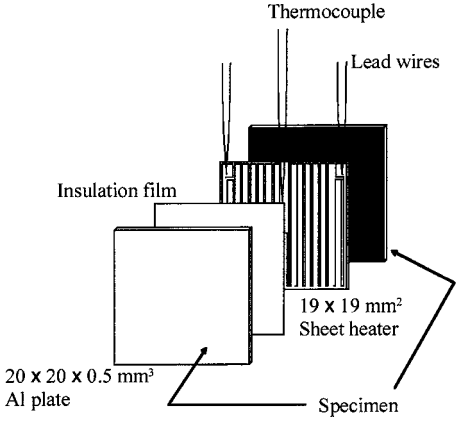


**Fig. 4.** Sample structure.

## 4. CALCULATION METHOD

Thermal control films are usually thin polymer films with vapor-deposited metal on the back surface as shown in Fig. 5. It is possible to produce thermal control films with the required values of $\varepsilon_h$ by selecting appropriate materials (polymer films and vapor-deposited metal) and an appropriate thickness for each layer. The present calculation method [8, 9] for the sample temperature dependence of $\varepsilon_h$ enables us to design suitable thermal control films which satisfy the target values of $\varepsilon_h$ and to predict the values in the temperature region in which they are difficult to measure experimentally.

This calculation method is performed according to the following procedures, using data for the optical constants of polyimide films and aluminum. In this calculation, it is assumed that each layer is homogeneous, nonscattering, and smooth, with no temperature dependence of its optical constants. The polyimide film/aluminum combination is assumed to be opaque, thus the total transmittance is not included in these calculations.

First, the optical constants of polyimide films are obtained from measurements of their normal spectral reflectance and transmittance. The normal spectral reflectance and transmittance are measured by a Fourier transform spectrometer (Bio-Rad FTS-60A/896) in the wavelength region from 0.25 to 100 μm. For example, the optical constants of UPILEX-S film are shown in Fig. 6. The optical constants of aluminum are obtained from a handbook [10].

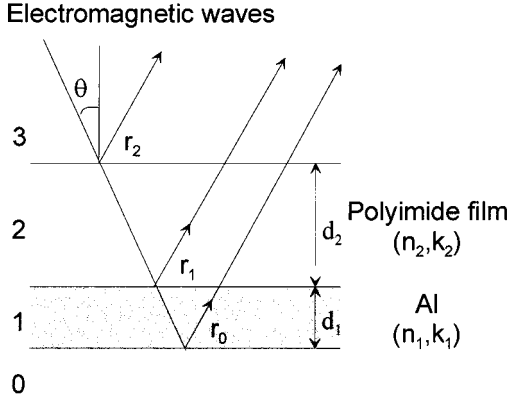


**Fig. 5.** Calculation model for thermal control films.

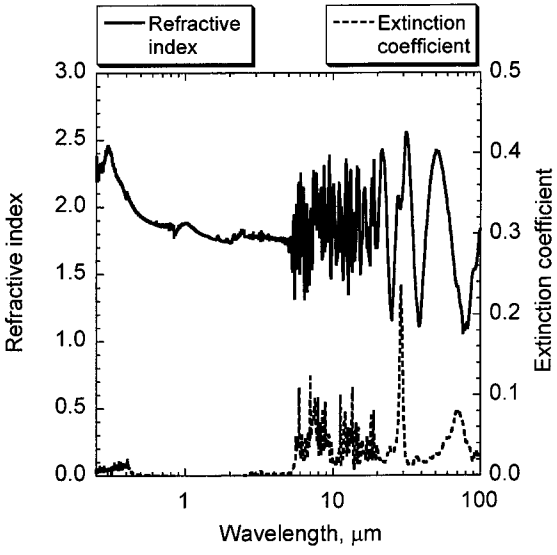


**Fig. 6.** Optical constants of UPILEX-S.

Amplitude reflectances of thermal control films are calculated from the optical constants of polyimide films and aluminum, and then the spectral reflectance is calculated with amplitude reflectances. The calculation is made for two cases: with and without consideration of an interference phenomenon. Since the interference phenomena of polyimide films are strong in the wavelength region from 2.5 to 20 μm, which has been confirmed in measurements of normal spectral reflectance and transmittance of polyimide films, they are considered in calculating the amplitude reflectance and spectral reflectance.

When interference is not considered, spectral reflectances account for multiplex reflectance at the boundary surface between the $m$th and the $(m+1)$th layers from the bottom and are expressed by

$$R'_m(\lambda, \theta) = r_m + \frac{(1-r_m)^2 R'_{m-1}(\lambda, \theta) \exp(-2\gamma_m d_m)}{1-r_m R'_{m-1}(\lambda, \theta) \exp(-2\gamma_m d_m)} \tag{3}$$

where $\gamma_m = 4\pi k_m / \lambda \cos \theta_m$, $r_m = (|r_{Sm}|^2 + |r_{Pm}|^2)/2$, $r_{Sm}$ and $r_{Pm}$ are the Fresnel coefficients, $k_m$ is the extinction coefficient of the $m$th layer, $\theta_m$ is the incident angle of electromagnetic waves of the $m$th layer, and $d_m$ is the thickness of the $m$th layer. Thus, the spectral reflectance of the surface of

the thermal control film as a function of the incident angle and the wavelength is expressed by

$$R(\lambda, \theta) = r_{ma} + \frac{(1-r_{ma})^2 R'_{ma-1}(\lambda, \theta) \exp(-2\gamma_{ma} d_{ma})}{1-r_{ma} R'_{ma-1}(\lambda, \theta) \exp(-2\gamma_{ma} d_{ma})} \tag{4}$$

where the subscript $ma$ indicates the layer number.

On the other hand, when interference is considered, amplitude reflectances which take into account multiplex reflectance at the boundary surface between the $m$th and the $(m+1)$th layers from the bottom are expressed by

$$R''_m(\lambda, \theta) = \frac{r_m + R''_{m-1}(\lambda, \theta) \exp(-i\eta_m)}{1+r_m R''_{m-1}(\lambda, \theta) \exp(-i\eta_m)} \tag{5}$$

where $\eta_m = 4\pi \hat{n}_m d_m \cos\theta_m / \lambda$ and $\hat{n}_m$is the complex refractive index of the $m$th layer. Thus, the spectral reflectance of the surface of the thermal control film as a function of the incident angle and the wavelength is expressed by

$$R(\lambda, \theta) = \frac{|R''_{Sma}(\lambda, \theta)|^2 + |R''_{Pma}(\lambda, \theta)|^2}{2} \tag{6}$$

where $R''_{Sma}(\lambda, \theta)$ and $R''_{Pma}(\lambda, \theta)$ are the spectral reflectances of S-polarization and P-polarization of the surface of the thermal control film from Eq. (5), respectively. In this way, the spectral reflectance $R(\lambda, \theta)$of the surface of the thermal control film is obtained by using Eq. (4) or (6).

Finally, the temperature dependence of $\varepsilon_h$ is calculated by integration of the spectral reflectance in the wavelength region from 0.25 to 100 μm and in the incident angle of electromagnetic waves from 0 to $\pi/2$, expressed by

$$\varepsilon_h = \frac{\int_0^{\pi/2} \int_{0.25}^{100} \{1-R(\lambda, \theta)\} i_b(\lambda, T) \cos\theta \sin\theta \, d\lambda \, d\theta}{\int_0^{\pi/2} \int_{0.25}^{100} i_b(\lambda, T) \cos\theta \sin\theta \, d\lambda \, d\theta} \tag{7}$$

where $T$ is the sample temperature and $i_b(\lambda, T)$ is Planck's spectral distribution of emissive power. It is possible to ignore the difference between the calculated result and the theoretical value over a restricted wavelength region, as about 97.9% of the emissive power of the blackbody is contained at 173.15 K, and approximately 100.0% at 700 K, in this wavelength region. And in Eq. (7), Lambert's cosine law is used to convert the normal emissive power into the directional emissive power.

## 5. RESULTS AND DISCUSSION

In the present experimental measurements of $\varepsilon_h$ in the temperature range from 173.15 to 523.15 K, the main factors of the uncertainty are considered to be as follows: variations of the supplied electrical power $Q$, measurements of the surface area of specimens $A_S$, and temperature measurements $T_S$ and $T_W$. The terminal voltage and the electric current, which determine the supplied electrical power, are measured by a digital multimeter with an accuracy of $\pm 0.11\%$. The estimated uncertainty of the surface area of the specimen is within $\pm 1.0\%$. And the uncertainty of the temperature measurements is estimated to be within $\pm 0.32$ K in this temperature range. Therefore, the overall uncertainty of the present experimental measurements of $\varepsilon_h$ is estimated to be at most $\pm 1.5\%$ in the temperature range. As for the temperature range from 523.15 to 700 K, the uncertainty of the temperature measurements is estimated to be within $\pm 0.62$ K. The heat loss of the sample through the lead wires $Q_W$ is not considered in calculating $\varepsilon_h$ according to Eq. (2). This contributes less than 3% to the uncertainty of $\varepsilon_h$, which is estimated by the heat conduction analysis. The uncertainties of measurements of the supplied electrical power and the surface area of the specimen are the same as mentioned above. Consequently, the overall uncertainty of the present experimental measurement of $\varepsilon_h$ is estimated to be at most $+1.5$ and $-3.5\%$ in the temperature range from 523.15 to 700 K.

The uncertainty of the present calculated results is believed to be due mainly to the uncertainty of the optical constants and the thicknesses of polyimide films. The uncertainty in the optical constants is estimated to be less than $\pm 5\%$, which corresponds to the experimental results for the spectral reflectance and transmittance of polyimide films. The uncertainty of the thickness of polyimide films is estimated to be less than $\pm 5\%$. In consequence, the overall uncertainty of the present calculated results of $\varepsilon_h$ is within $+3.5\%$ and $-5.0\%$.

Figure 7 shows comparisons of the experimental and calculated results for the temperature dependence of $\varepsilon_h$ for aluminum-deposited UPILEX-S films (20 μm), aluminum-deposited UPILEX-R films (25 μm), and aluminum-deposited Kapton-H films (25 μm).

As for the $\varepsilon_h$ of aluminum-deposited UPILEX-S films at low temperatures and aluminum-deposited UPILEX-R films at high temperatures, the maximum difference between experimental and calculated results is 0.05 to 0.07. This is because the calculated optical constants of polyimide films are not correctly obtained, resulting from different orientations of polyimide films between sample specimens. In the other temperature region, however, the calculated results agree very well with the experimental results. According to these comparisons, it has been demonstrated that this

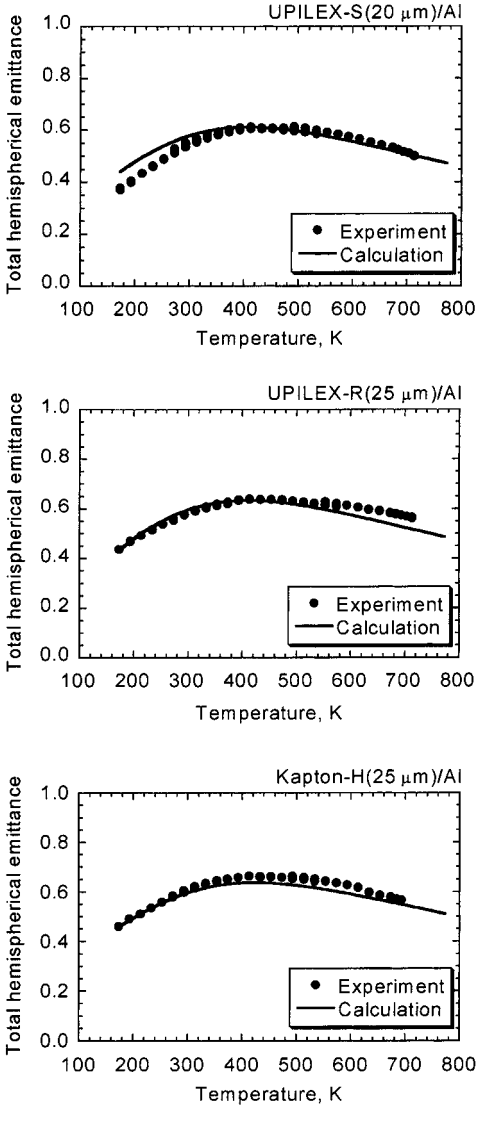


**Fig. 7.** Total hemispherical emittance of thermal control films.

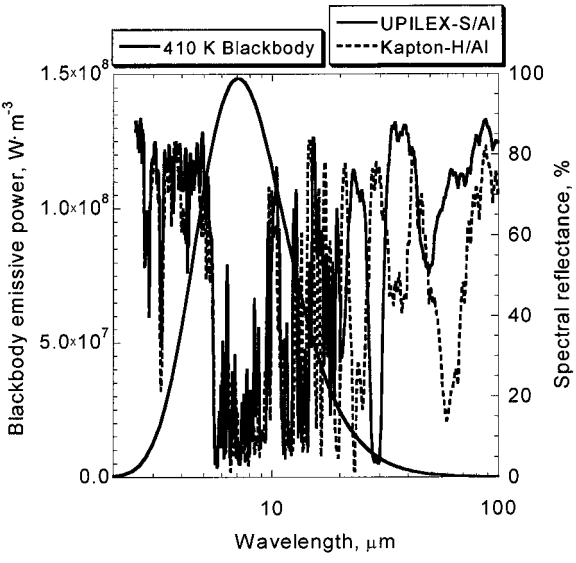


**Fig. 8.** Spectral reflectance of thermal control films.

present calculation method is an effective means to predict the temperature dependence of $\varepsilon_h$ in the temperature range from 173.15 to 700 K.

From these experimental measurements and calculations in the temperature range from 173.15 to 700 K, it has been observed that the temperature dependence of $\varepsilon_h$ of thermal control films is remarkable and the values have a maximum around 410 K. The reason why the values have a maximum around 410 K can be thought as follows. It is because the thermal control film has a low reflectance, that is, a high absorptance, in the wavelength region from 6 to 10 μm, which agrees with the wavelength at which the emissive power from a blackbody at around 410 K is at a maximum as shown in Fig. 8.

## REFERENCES

1. H. Saito, H. Yamakawa, Y. Kobayashi, and T. Mukai, IAF-98-Q.2.04 (1998).
2. R. Grard, G. Scoon, and M. Coradini, *ESA J.* **18**:197 (1994).
3. M. M. Finckenor and D. Dooling, NASA/TP-1999-209263 (1999).
4. A. Ohnishi and R. Sato, *Trans. IEE Japan* **116-A(2)**:136 (1996) (in Japanese).
5. H. Inoue, H. Okamoto, and Y. Hiraoka, *Int. J. Radiat. Appl. Instrum. Part C* **29**:283 (1987).
6. H. Yamane, *Polyimides: Characterization and Application: Proc. Second Int. Conf. Polyimides* (UMI, Ann Arbor, MI, 1989), pp. 86–105.

7. A. Ohnishi, T. Hayashi, and H. Nagano, *Proc. 4th Japan Symp. Thermophys. Prop.*, Vol. 1 (1983) (in Japanese).
8. R. Horikoshi, Y. Nagasaka, and A. Ohnishi, *Int. J. Thermophys.* **19**:547 (1998).
9. R. Siegel and J. R. Howell, *Thermal Radiation Heat Transfer*, 3rd ed. (Taylor and Francis, Washington, DC, 1992), pp. 11–91.
10. *American Institute of Physics Handbook*, 3rd ed. (McGraw–Hill, New York, 1972), pp. 6–124.